

Complete Gas-Phase Proton Microaffinity Analysis of Two Bulky Polyamine Molecules

Sadegh Salehzadeh,* Mehdi Bayat, and Mehdi Hashemi

Faculty of Chemistry, Bu-Ali Sina University, Hamedan, Iran

Received: April 13, 2007; In Final Form: June 7, 2007

Density functional theory (DFT) and ab initio (Hartree–Fock) calculations employing the 6-31G* basis set are used to determine gas-phase proton microaffinities ($PA_{n,i}$) of two bulky symmetrical tripodal tetraamine ligands $N[(CH_2)_4NH_2]_3$, trbn, and $N[(CH_2)_5NH_2]_3$, trpa. The corresponding proton macroaffinities (\overline{PA}_n) are calculated not only according to our recently established method but also considering two alternative formulas based on a Boltzmann distribution. The successive protonation macroconstants in aqueous solution for these bulky amines are predicted from the well-defined correlation between the calculated proton macroaffinities, without considering Boltzmann distribution, and the corresponding $\log K_n$ for these amines. The overall protonation constants are also predicted by two different methods.

1. Introduction

It is now well-established that electronic structure calculations provide accurate gas-phase proton affinities as well as valuable information on the structure of a base and its conjugate acid.¹ The proton affinity of a monobasic neutral ligand at 0 K is defined as the negative of the electronic energy difference between HL^+ and L together with a correction for difference in zero point energies. To convert the 0 K value to 298 K, one has to include thermal corrections for the translational, rotational, and vibrational energies and a correction for the change in the number of molecules assuming ideal gas behavior.²

Obviously for each polybasic molecule there may be several ways for protonation depending on which site is protonated. Protonation of different sites will release different amounts of energy. Therefore the incorrect term “proton affinity” for protonation of a special site on a polybasic molecule can be replaced by “proton microaffinity”, which we recently used for gas-phase protonation of polybasic molecules.³ We also applied two other types of defined gas-phase proton affinities for such molecules: proton macroaffinity and proton overall affinity. The proton macroaffinity of a polybasic molecule corresponds to its protonation macroconstant in solution. We established an equation, eq 1, for calculation of proton macroaffinities, \overline{PA}_n , of polyamine molecules with any type of symmetry.³

$$\overline{PA}_n = \frac{\sum_{j=1}^l \sum_{i=1}^m PA_{n,i} R_{n,j} S_{n,i}}{\sum_{j=1}^l \sum_{i=1}^m R_{n,j} S_{n,i}} \quad (1)$$

where

$$R_{n,j} = \sum_{j=1}^K R_{n-1,j} S_{n-1,j}$$

This formula shows that \overline{PA}_n not only depends on the proton microaffinities, $PA_{n,i}$, and the relative abundance of the species which is related to them, $R_{n,j}$, but also on the available identical

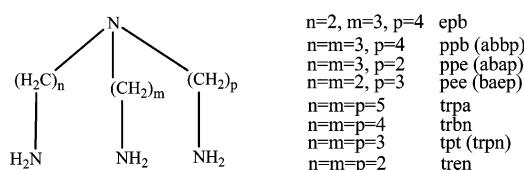


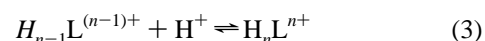
Figure 1. Structures of the tripodal tetraamine ligands investigated here along with their common abbreviations.

sites that undergo protonation, $S_{n,i}$. Obviously the relative abundance of the initial neutral molecule, $R_{1,1}$, is 1, and that of any other species depends on both the relative abundance of previous species, $R_{n-1,j}$, and the available identical sites on them, $S_{n-1,j}$, which are involved in its formation.

The proton overall affinity, PA_{ov} , is also defined as the negative of the electronic energy difference between L and its fully protonated form (herein H_4L^{4+}) together with a correction for difference in zero point energies. According to Hess's law the summation of the calculated proton macroaffinities for one polybasic molecule (\overline{PA}_{ov} ; see eq 2) must be the same as or very close to its PA_{ov} .

$$\overline{PA}_{ov} = \sum_{n=1}^m \overline{PA}_n \quad (2)$$

For first time, we have shown that there is a good correlation between the calculated gas-phase proton macroaffinities and the corresponding solution–protonation macroconstants (K_n ; see eqs 3 and 4) for a number of tripodal tetraamines (see Figure 1; tren, pee, ppe, tpt, and ppb) that in recent years have been interesting to us.^{3–8} Furthermore the correlation between the calculated $\log \overline{PA}_{ov}$ and measured $\log \beta_4$ (see eq 5) was really excellent for the latter tetraamines.



$$K_n = \frac{[H_nL^{n+}]}{[H_{n-1}L^{(n-1)+}][H^+]} \quad (4)$$

$$\beta_n = K_1 K_2 \dots K_n \quad (5)$$

* Corresponding author. Fax: +98(811)8257407. E-mail: saleh@basu.ac.ir.

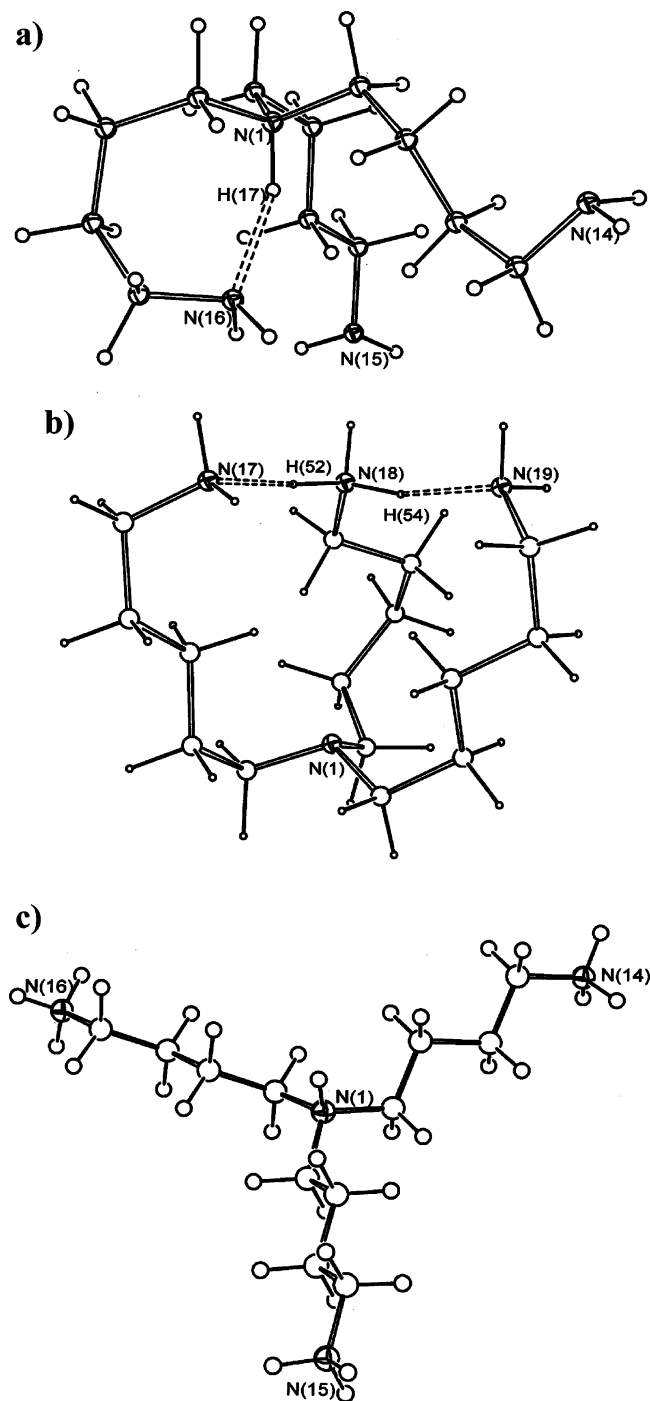


Figure 2. Calculated molecular structure of three protonated species studied here: Htrbn⁺ (a), Htrpa⁺ (b), and H₄trbn⁴⁺ (c).

We were interested in investigating whether our definitions for proton affinities of polybasic molecules are reliable for more bulky polybasic molecules. On the other hand, as can be seen, in our previous method we have not considered the Maxwell–Boltzmann equation (eq 6) for calculation of probability distribution (x_i) of different n protonated species.

$$x_i = \frac{e^{-\Delta G_i^*/RT}}{\sum_{i=1}^n e^{-\Delta G_i^*/RT}} \quad (6)$$

Thus in this work we extend our complete gas-phase proton microaffinity analysis to two bulky symmetrical tetraamine

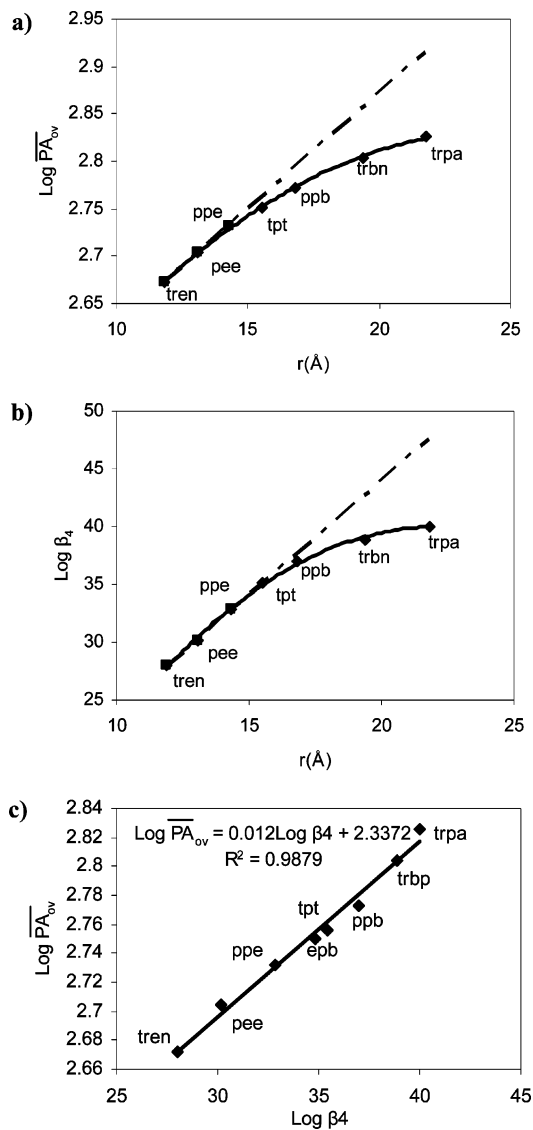
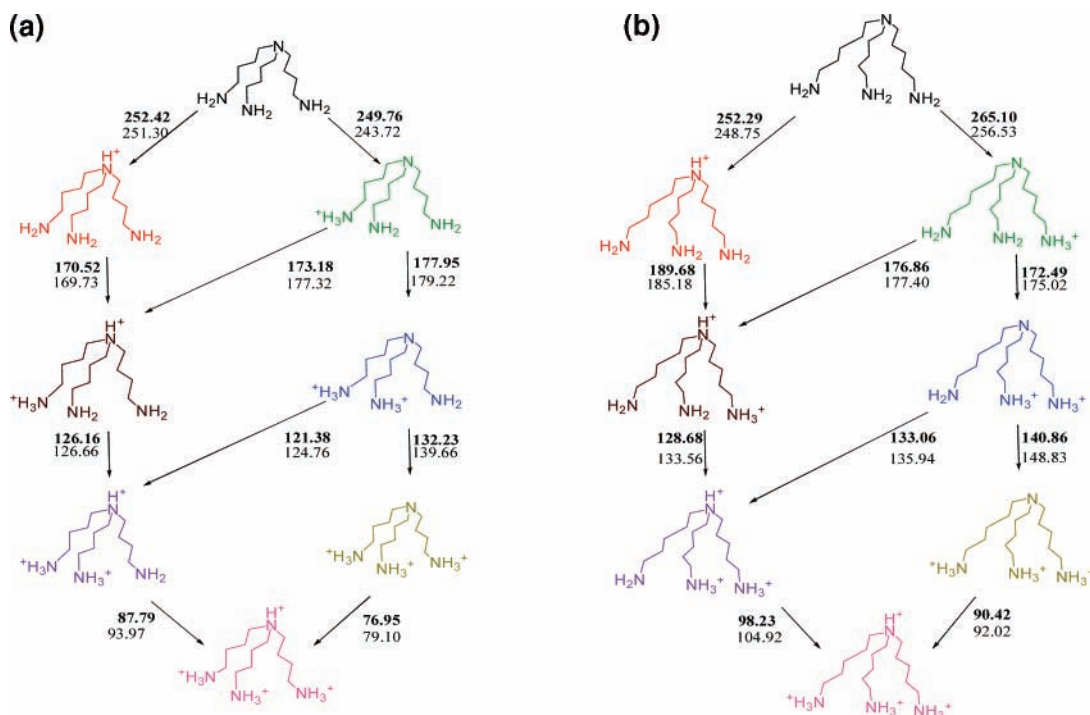


Figure 3. $\log \overline{PA}_{ov}$ (a) and $\log \beta_4$ (b) versus the sum of the lengths of the three aliphatic chains in each tripodal tetraamine, r . Correlation of $\log \beta_4$ and calculated $\log \overline{PA}_{ov}$ for all tripodal tetraamines discussed here at B3LYP/6-31G* level of theory (c).

ligands $N[(CH_2)_4NH_2]_3$, trbn,⁹ and $N[(CH_2)_5NH_2]_3$, trpa¹⁰ (Figure 1). We show the effect on the proton macroaffinities of these types of tripodal ligands by considering the Maxwell–Boltzmann distribution for differently protonated species. We also predict the solution–protonation macroconstants and overall protonation constants for these molecules. The gas-phase proton affinities are calculated by both the ab initio Hartree–Fock (HF) theory and density functional theory (DFT).

2. Computational Methods

The geometries of all species in the gas phase were fully optimized at both the Hartree–Fock and DFT (B3LYP)¹¹ levels of theory using the Gaussian 98 set of programs.¹² The standard 6-31G* basis set was used for all calculations. Vibrational frequency analysis, calculated at the same level of theory, indicates that optimized structures are at the stationary points corresponding to local minima without any imaginary frequency. Calculations were performed on a Pentium-PC computer with 3000 MHz processor. A starting molecular-mechanics structure for the ab initio calculations was obtained using the HyperChem 5.02 program.¹³ Calculated Cartesian atomic coordinates of the

SCHEME 1: Illustration of All Possible Paths for Gas-Phase Protonation of Ligand trbn (a) and trpa (b) along with Calculated Proton Microaffinities (kcal/mol) at Both the B3LYP and HF/6-31G* Levels of Theory^a

^a The data obtained at the HF/6-31G* level are given as plain text; those for the B3LYP/6-31G* level are in Bold.

optimized standard orientation for all species are given in the Supporting Information. The results of DFT calculations are presented here, and those of HF calculations are given in Supporting Information.

3. Results and Discussion

The number of proton microaffinities in the complete protonation of polybasic molecules depends not only upon the number of basic sites but also upon the symmetry of the molecule. The two tripodal tetraamines investigated here, trbn and trpa, belong to the general type A_3B . It has been mathematically shown that for the protonation of such molecules in solution there are 8 different microspecies as well as 10 microconstants.¹⁴ The successive protonation steps of trbn and trpa are shown in Scheme 1. In this scheme the 8 different microspecies for each tetraamine are illustrated as 8 different colors and proton microaffinities are calculated as we recently described³ according to the energies of the related microspecies (see Supporting Information, Tables S1 and S2). It is well-known that the proton affinity of amines may be affected by intra-hydrogen bonding.^{15,16} The optimized structures of protonated species of trbn and trpa, except the fully protonated species, always show intra-hydrogen bonding. The molecular structure of some protonated species are shown in Figure 2. As can be seen, intra-hydrogen-bonding exists where either the tertiary or primary amine is protonated (see Figure 2a,b). On the other hand, as would be expected, in the case of fully protonated species the ligands always tend to adopt a “splayed” arrangement of the ligand arms due to electrostatic effects (see Figure 2c). A similar structure has been confirmed for tetra-protonated derivatives of tren in the solid state.^{17,18}

After computation of all proton microaffinities, we used eq 1³ and two newly defined eqs 7 and 8 to calculate the proton macroaffinities, PA_n .

$$\text{PA}_n = \frac{\sum_{i=1}^n \text{PA}_{n,i} x_i}{\sum_{i=1}^n x_i} \quad (7)$$

$$\text{PA}_n = \frac{\sum_{j=1}^l \sum_{i=1}^m \text{PA}_{n,i} R_{n,j} S_{n,i} x_i}{\sum_{j=1}^l \sum_{i=1}^m R_{n,j} S_{n,i} x_i} \quad (8)$$

In the latter two equations, in contrast to eq 1, the population of the various species (x_i) is considered; this is evaluated from the computed Gibbs energies through a Boltzmann distribution¹⁵ according to eq 6. While in the case of eq 7 the proton macroaffinities are calculated mainly according to a Boltzmann distribution, in eq 8 the latter distribution is added to eq 1. For calculation of proton macroaffinities in each protonation step of the amine, in the case of eq 7, all proton microaffinities in that step and the population of the related species (calculated using eq 6) are considered. On the other hand, in the case of eq 8, in addition to all proton microaffinities and the population of the related species the parameters included in eq 1 are also considered. The proton overall affinities were also calculated as the negative of the electronic energy difference between L and its fully protonated form together with a correction for differences in zero point energies. The summation of calculated proton macroaffinities, PA_{ov} , for these amines, using eq 1

TABLE 1: Comparison of Gas-Phase Proton Macroaffinities (kcal/mol), \overline{PA}_n , and Proton Overall Affinities for Tripodal Tetraamines^a

| | tren | pee | ppe | Tpt | ppb | trbn | trpa |
|----------------------|---------------|---------------|---------------|---------------|---------------|---------------|---------------|
| \overline{PA}_1 | 220.42 | 224.69 | 233.30 | 237.84 | 240.08 | 252.26 | 251.37 |
| | 219.57 | 224.23 | 231.60 | 235.19 | 240.38 | 251.99 | 252.37 |
| | <i>222.00</i> | <i>225.30</i> | <i>231.00</i> | <i>235.80</i> | <i>243.60</i> | <i>250.40</i> | <i>261.90</i> |
| \overline{PA}_2 | 145.55 | 149.20 | 144.62 | 165.87 | 170.00 | 172.38 | 183.26 |
| | 147.22 | 147.69 | 149.67 | 165.88 | 167.17 | 172.38 | 183.25 |
| | <i>154.60</i> | <i>159.20</i> | <i>164.40</i> | <i>165.70</i> | <i>169.40</i> | <i>174.90</i> | <i>177.90</i> |
| \overline{PA}_3 | 77.29 | 90.07 | 94.10 | 100.86 | 120.46 | 132.00 | 137.00 |
| | 77.29 | 90.07 | 94.10 | 100.86 | 120.46 | 132.00 | 137.00 |
| | <i>84.00</i> | <i>93.80</i> | <i>101.20</i> | <i>107.60</i> | <i>113.60</i> | <i>126.50</i> | <i>132.80</i> |
| \overline{PA}_4 | 18.41 | 32.05 | 50.83 | 67.50 | 58.46 | 77.26 | 93.24 |
| | 18.41 | 32.05 | 50.83 | 67.50 | 58.46 | 77.26 | 93.24 |
| | <i>9.20</i> | <i>28.20</i> | <i>42.40</i> | <i>61.70</i> | <i>66.20</i> | <i>85.08</i> | <i>96.30</i> |
| \overline{PA}_{ov} | 461.67 | 496.02 | 522.85 | 572.07 | 588.61 | 633.90 | 665.81 |
| | 462.50 | 494.04 | 526.19 | 569.44 | 588.16 | 633.63 | 665.86 |
| | <i>469.80</i> | <i>506.50</i> | <i>539.00</i> | <i>570.80</i> | <i>592.80</i> | <i>636.90</i> | <i>668.90</i> |
| PA_{ov} | 469.70 | 506.00 | 539.10 | 570.80 | 592.80 | 636.89 | 668.89 |

^a The \overline{PA}_n obtained from eq 7 and the corresponding \overline{PA}_{ov} are given as plain text, those from the eq 8 are in bold, and those from eq 1 are in italic.³ \overline{PA}_{ov} is calculated as the negative of the electronic energy difference between L and its fully protonated form (herein H_4L^{4+}) together with a correction for the difference in zero point energies. All calculations were performed at the B3LYP/6-31G* level of theory.

TABLE 2: Comparison of the Predicted Protonation Macroconstants^{a,b} for trbn and trpa with Measured Protonation Macroconstants^c for Other Polybasic Molecules Studied Here

| tim | log K_1 | log K_2 | log K_3 | log K_4 | log β_4 |
|------|--------------|--------------|--------------|-------------|---------------|
| tren | 10.14 | 9.43 | 8.41 | | 27.98 |
| pee | 10.22 | 9.52 | 8.78 | 1.61 | 30.13 |
| ppe | 10.38 | 9.68 | 8.95 | 3.81 | 32.82 |
| tpt | 10.51 | 9.82 | 9.13 | 5.62 | 35.08 |
| ppb | 10.69 | 10.12 | 9.49 | 6.72 | 37.02 |
| trbn | <i>10.81</i> | <i>10.27</i> | <i>9.80</i> | <i>7.88</i> | <i>38.76</i> |
| | 10.86 | 10.22 | 9.75 | 7.79 | 38.69 |
| trpa | <i>11.08</i> | <i>10.34</i> | <i>10.00</i> | <i>8.55</i> | <i>39.97</i> |
| | 11.13 | 10.34 | 9.91 | 8.49 | 39.87 |

^a The data obtained at the HF/6-31G* level are given as italic, those for the B3LYP/6-31G* level are in bold. ^b The data are derived from the correlation diagrams for proton macroaffinities calculated using eq 1 with corresponding protonation constants (see Supporting Information, Figure S1). ^c Reference 6.

alone, is always the same as or very close to the calculated proton overall affinities (Table 1).

Over the four steps of protonation the summation of the calculated proton macroaffinities using all three eqs 1, 7, and 8 gives the order of basicity as follows: trpa > trbn > ppb > tpt > epb > ppe > pee > tren (Table 1). This is the expected trend (increasing basicity with increasing number of methylene groups). On the other hand, as can be seen in Table 1, using eq 1 alone, we can consistently see the same trend for the calculated proton macroaffinities in all four individual steps of protonation of this series of molecules.

The correlation of log K_n and calculated log \overline{PA}_n for all four steps of complete protonation of the tren, pee, ppe, tpt, and ppb tripodal tetraamines was studied (see Supporting Information, Figures S1–3). The result showed that, using only eq 1, the correlations are very good for all four successive protonation steps. This observation has previously led us to predict the unknown stepwise protonation macroconstants for epb³ and now those for trbn and trpa (see Table 2).

Parts a and b of Figure 3 show the variations of log \overline{PA}_{ov} (calculated with eq 1) and log β_4 with increasing sum of the lengths of the three aliphatic chains ($r = \sum_{i=1}^3 r_i$, where r_i is defined as the distance of each terminal nitrogen atom from the central tertiary nitrogen atom) in each tripodal tetraamine,

respectively. It is interesting that the amount of increase becomes less as r increases (compare the straight dashed lines with the observed solid curves in Figure 3a,b). Obviously when r is short, the electrostatic repulsions between the positively charged nitrogen atoms are very high and increasing the size of r (for example from tren to pee) will significantly increase the basicity of the molecule. Furthermore, with increasing length of the aliphatic chains, the inductive effect of additional methylene groups will be decreased. We can see a similar result if we study the variations of measured protonation constants of a series of aliphatic diamines with increasing r .¹⁹

The good correlation of log β_4 and calculated log \overline{PA}_{ov} for tren, pee, ppe, tpt, epb, ppb, trbn, and trpa tripodal tetraamines is shown in Figure 3c. This similarity for reliable variations of log \overline{PA}_{ov} and log β_4 with increasing of r , as well as observation of very good correlation of log β_4 with calculated log \overline{PA}_{ov} , again supports our definition for both the proton macroaffinity and proton overall affinity.

The above results indicate that our previously defined equation (eq 1) for calculation of proton macroaffinities for this type of polybasic molecules is more reliable than other equations including the Boltzmann distribution.

4. Conclusion

The results of this work support our recent definitions for proton affinities of polybasic molecules. The reliable theoretical calculation of the gas-phase proton macroaffinities and proton overall affinities of polybasic molecules with any symmetry according to the complete proton microaffinity analysis is possible. The accurate prediction of corresponding basicity in solution according to calculation of related proton affinities is also potentially possible. The calculation of proton macroaffinities considering the Boltzmann distribution is also possible, but the results of this work show that for this type of polyamines it is less reliable.

Acknowledgment. Special thanks to Prof. R. V. Parish (Manchester University) for his help in improving our English.

Supporting Information Available: Tables of energies, Maxwell–Boltzmann distribution populations, proton affinities,

$\log K_n$ vs $\log \overline{PA}_n$ diagrams, $\log \overline{PA}_{ov}$ vs $\log \beta_4$, calculations of proton microaffinities, and Cartesian coordinates. This material is available free of charge via the Internet at <http://pubs.acs.org>.

References and Notes

- (1) Deakyne, C. A. *Int. J. Mass Spectrosc.* **2003**, 227, 601.
- (2) Rusted, J. R.; Dixon, D. A.; Kubicki, J. D.; Felmy, A. R. *J. Phys. Chem. A* **2000**, 104, 4051.
- (3) Salehzadeh, S.; Bayat, M. *Chem. Phys. Lett.* **2006**, 427, 455.
- (4) Salehzadeh, S.; Javarsineh, S. A.; Keypour, H. *J. Mol. Struct.* **2006**, 785, 54.
- (5) Salehzadeh, S.; Nouri, S. M.; Keypour, H.; Bagherzadeh, M. *Polyhedron* **2005**, 24, 1478.
- (6) Keypour, H.; Dehdari, M.; Salehzadeh, S. *Transition Met. Chem. (Dordrecht, Neth.)* **2003**, 28, 425.
- (7) Keypour, H.; Salehzadeh, S.; Pritchard R. G.; Parish, R. V. *Inorg. Chem.* **2000**, 39, 5787.
- (8) Keypour, H.; Salehzadeh, S. *Transition Met. Chem. (Dordrecht, Neth.)* **2000**, 25, 204.
- (9) Niitsu, M.; Sano, H.; Samejima, K. *Chem. Pharm. Bull.* **1992**, 40, 2958.
- (10) Weigert, F. J. *J. Org. Chem.* **1978**, 43, 622.
- (11) Becke, A. D. *J. Chem. Phys.* **1993**, 98, 5648.
- (12) Frisch, M. J.; Trucks, G. W.; Schlegel, H. B.; Scuseria, G. E.; Robb, M. A.; Cheeseman, J. R.; Montgomery, J. A., Jr.; Vreven, T.; Kudin, K. N.; Burant, J. C.; Millam, J. M.; Iyengar, S. S.; Tomasi, J.; Barone, V.; Mennucci, B.; Cossi, M.; Scalmani, G.; Rega, N.; Petersson, G. A.; Nakatsuji, H.; Hada, M.; Ehara, M.; Toyota, K.; Fukuda, R.; Hasegawa, J.; Ishida, M.; Nakajima, T.; Honda, Y.; Kitao, O.; Nakai, H.; Klene, M.; Li, X.; Knox, J. E.; Hratchian, H. P.; Cross, J. B.; Adamo, C.; Jaramillo, J.; Gomperts, R.; Stratmann, R. E.; Yazyev, O.; Austin, A. J.; Cammi, R.; Pomelli, C.; Ochterski, J. W.; Ayala, P. Y.; Morokuma, K.; Voth, G. A.; Salvador, P.; Dannenberg, J. J.; Zakrzewski, V. G.; Dapprich, S.; Daniels, A. D.; Strain, M. C.; Farkas, O.; Malick, D. K.; Rabuck, A. D.; Raghavachari, K.; Foresman, J. B.; Ortiz, J. V.; Cui, Q.; Baboul, A. G.; Clifford, S.; Cioslowski, J.; Stefanov, B. B.; Liu, G.; Liashenko, A.; Piskorz, P.; Komaromi, I.; Martin, R. L.; Fox, D. J.; Keith, T.; Al-Laham, M. A.; Peng, C. Y.; Nanayakkara, A.; Challacombe, M.; Gill, P. M. W.; Johnson, B.; Chen, W.; Wong, M. W.; Gonzalez, C.; Pople, J. A., Jr. *Gaussian 03*, Revision B.04; Gaussian, Inc.: Pittsburgh, PA, 1998.
- (13) *Hyper Chem*, Release 5.02; Hypercube, Inc.: Gainesville, FL, 1997.
- (14) Szakác, Z.; Noszál, B. *J. Math. Chem.* **1999**, 26, 139.
- (15) Wang, Z.; Michael, K. W.; Siu, et al. *J. Phys. Chem. A* **1999**, 103, 8700.
- (16) Kone, S.; Galland, N.; Le Questel, J. Y.; et al. *Chem. Phys.* **2006**, 328, 307.
- (17) Blackman, A. G. *Polyhedron* **2005**, 24, 1.
- (18) Ilioudis, C. A.; Hancock, K. S. B.; Georganopoulou, D. G.; Steed, J. W. *New J. Chem.* **2000**, 24, 787.
- (19) Cascio, S.; Robertis, A. D.; Foti, C. *J. Chem. Eng. Data* **1999**, 44, 735.